International Journal of Advanced Geosciences, 13 (2) (2025) 1-12

International Journal of Advanced Geosciences

Website: www.sciencepubco.com/index.php/IJAG
https://doi.org/10.14419/212zmm85
Research paper

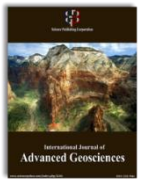

Investigation of Climate Fluctuations Through Analysis of Meteorological Data and Forecasting in Port Harcourt, Nigeria

Emmanuel M. Menegbo [1] *, Jackson Peace Kurotamuno [2]

[1] Department of Surveying and Geoinformatics, Captain Elechi Amadi Polytechnic Rumuola, P.M.B 5936, Port Harcourt, Rivers State, Nigeria
[2] Department of Surveying and Geomatics, Rivers State University, Nigeria
**Corresponding author E-mail: nenibarini@yahoo.com*

Received: June 18, 2025, Accepted: August 10, 2025, Published: August 16, 2025

Abstract

The research on studying and predicting climatic phenomena in Port Harcourt, Nigeria, has evolved based on the vast knowledge and information collected. This has greatly improved the understanding and prediction of weather changes in the region. In addition to traditional climate change indicators like temperature, wind, humidity, clouds, and rainfall, this study also explores the variability of global radiation. The primary objective of this research was to assess climate variability using meteorological parameters and forecasting in Port Har-court, Rivers State, Nigeria. The study utilized data from the Meteonorm Version 8 database archives to analyze radiation, temperature, and precipitation trends. The Standard interpolation method (Shepard's gravity interpolation model) was employed to obtain the data. Stochastic models and the Perez tilt radiation model were used to examine climate data from 1972–1991, 1965–1989, and 2020 and 2050. Results indicate a yearly Temperature average of 26.3°C between 1972 and 1991 and a projected value of 27.6°C in 2050. Furthermore, the analysis shows a decreasing trend in precipitation in Port Harcourt, with the maximum value expected to decrease to 323mm in 2050 from 400mm observed between 1972–1991. The projected global radiation levels are expected to reach 1722kWh/m2 by 2050, up from 1476kWh/m2 recorded between 1965 and 1989. It is strongly advised to consider data from various locations in Port Harcourt and Nigeria, as well as the local climatic characteristics, for future study. The study is useful for selecting suitable sites for green energy projects like solar power stations and wind farms.

Keywords: *Climatic Change; Meteorological Data; Forecasting; Meteonorm 8 and Port Harcourt.*

1. Introduction

Meteorological data parameters related to climate change, such as radiation, temperature, and precipitation, are considered key environmental factors. Research conducted by Semenza and Ebi (2019) suggests that temperature and precipitation have the most substantial impact on migration patterns. Various studies, including Cai et al. (2016), have highlighted the multiple ways in which temperature and precipitation can influence human behaviors. Among these factors, the connection between migration and climate change is primarily driven by changes in agricultural productivity.

From a broader standpoint, Bohra-Mishra et al. (2014) have illustrated the connection between climate change and outward migration. While precipitation is significant, the rise in temperatures appears to have a unique impact. Specifically, temperature has a nonlinear relationship with migration, with temperatures above 25°C being linked to an uptick in outmigration, possibly due to its influence on economic factors.

However, in contrast, decreases in rainfall (related to droughts) or increases in rainfall (related to floods) can both potentially increase migration in a particular area. While precipitation also affects migration in a nonlinear way, its impact is not as significant as temperature. It seems that sudden extreme events caused by heavy precipitation result in lower permanent migration compared to the gradual effects of climate change driven by temperature rise. Floods may force communities to relocate temporarily, but they often return permanently.

Meteorologists prioritize precipitation point temperature over relative humidity to gauge individual comfort and forecast rainfall, ice, smog formation, and storm likelihood (Yousif and Tahir 2013). When the dew point in the lower stratosphere exceeds 60°C, violent rainstorms are possible (Ukhurebor et al. 2017). Numerous surveys have been conducted around the world to track current temperature and solar radiation trends. In local climates, various factors beyond temperature play a significant role in shaping environmental climatic patterns, showing longitudinal and earthly variations (Frimpong et al. 2014).

This leads to a scarcity of ground-based weather stations in many countries. Studies have indicated that data collected from ground-based sources can be a reliable and consistent source of atmospheric information for climate studies. Aweda and Samson (2020) made predictions about future temperature trends in Nigeria. Utilizing statistical tools and methodologies is crucial for accurately forecasting air temperature,

Copyright © Emmanuel M. Menegbo, Jackson Peace Kurotamuno. This is an open access article distributed under the Creative Commons Attribution License, which permits unrestricted use, distribution, and reproduction in any medium, provided the original work is properly cited.

as highlighted by Murat et al. (2018). Time series forecasting methods rely on analyzing past data patterns, as noted by various scholars, including Murat et al. (2018). It is widely recognized that historical data trends can be utilized to project future occurrences.

Advancements in weather forecasting techniques over the centuries have led to a wealth of knowledge and data that are instrumental in understanding and predicting climate change, a phenomenon that significantly influences atmospheric research worldwide. The soil-plant-atmosphere system is being affected by the ongoing global warming process, necessitating accurate predictions of future weather patterns and an anticipated rise in the frequency and intensity of extreme events (Semenov and Shewry, 2011). Studies by Lobell et al. (2013) have identified rising temperatures and reduced precipitation as key contributors to the prevalence of droughts due to global warming, posing significant challenges to global food security. Additionally, research by Ukhurebor et al. (2017) has highlighted the positive impact of climate change on life expectancy and overall well-being.

The position, elevation, and closeness to bodies of water are all influenced by the latitude of a particular location. Solar irradiation has proven to be a key factor in studying climate adjustments, environmental impacts, crop yields, food resources, and water systems (Pondyal et al. 2012). However, when designing a solar power system, it is essential to have a thorough understanding of the availability of solar radiation worldwide in interest (Aweda and Samson 2020). Consequently, the capability of solar radiation plays a crucial role in predicting atmospheric variables (Poudyal et al. 2012).

The IPCC Sixth Assessment Report (AR6) provides a stark warning about the accelerating pace of climate change and its disproportionate impacts on vulnerable regions. For West Africa and other tropical areas, AR6 projects a continued increase in mean temperatures, exceeding the global average in many parts (IPCC, 2021). These variables play a crucial role in determining climate variations and weather conditions. Drastic climate changes have a significant impact on both the environment and human infrastructure, surpassing typical expectations(Rebetez, 2001). In addition, the ability to adapt to different climates is a key consideration for human well-being. (Geerts, 2003).

Various approaches have been employed in time series analysis, including the use of autoregressive integrated moving-average (ARIMA) models for forecasting temperature patterns. Muhammet (2012) applied the ARIMA methodology to predict temperature and precipitation trends in Afyonkarahisar Province, Turkey, up to the year 2025. The results indicated that both quadratic and linear trend models suggested a temperature rise. Additionally, Khedhiri (2014) examined the statistical characteristics of historical temperature data in Canada spanning from 1913 to 2013. A seasonal ARIMA model was developed to forecast future temperature fluctuations. Through the utilization of SARIMA models, Afrifa-Yamoah (2016) projected monthly rainfall levels in various regions within Ghana.

This study utilizes Meteonorm desktop version 8.0 to access and analyze meteorological satellite data to interpolate radiation, precipitation, and temperature on a global scale. The methodology employed for processing the satellite images is based on techniques like Heliosat II (Lefèvre et al., 2002). Hourly visible channel images from geostationary satellites, including MSG (2008-2020), Himawari (2019-2020), GOES-E (2018-2019), and Indoex, have been utilized. The satellite data is transformed into daily averages for global radiation, precipitation, and temperature, which are then aggregated to generate monthly statistical values and forecasts.

The Meteonorm desktop version 8.0 includes various international databases. Global radiation data were sourced from the GEBA Global Energy Balance Archive (WMO World Climate Program - Water) (Gilgen et al., 1998) and underwent quality control through six distinct procedures (physical probability checks, time series analysis, and cloud data comparison). Temperature, humidity, wind data, sunshine duration, and days with precipitation were cross-referenced with WMO Climatological Normals 1961–1990 (WMO, 1998). To address missing data and ensure uniform distribution of weather station information, additional databases such as the data summary of international weather stations compiled by the National Climatic Data Center, USA (NCDC, 1995/2002) were integrated.

The climate change data in the updated Meteonorm version 8 is derived from the IPCC report 2014 (AR5) scenarios, specifically the Representative Concentration Pathways (RCP) RCP2.6 (low), RCP4.5 (mid), and RCP8.5 (high). Models were averaged for the periods 2011-2030, 2046-2065, and 2080-2099, with linear interpolation for years in between. This allows for accurate data representation for future years, ranging from 2020 to 2100, in Meteonorm 8 for user selection. By utilizing the Meteonorm Version 8 database, solar energy systems can be effectively simulated across global regions with a high level of consistency. The interpolation errors typically fall within the range of climate fluctuations from year to year.

1.1. Meteorological models used in Meteonorm version 8 database

Zelenka et al. (1992) propose that to calculate meteorological data for any location worldwide using Meteonorm 8, an interpolation method is necessary. The interpolation for global radiation specifically involves the use of a 3-D inverse distance model, known as Shepard's gravity interpolation. Additionally, a North-South distance penalty must be factored in, as stated by Wald and Lefèvre (2001). Where

$Gh(x) = \sum w_i .[Gh(x_i) + (z_i - z_x) .g_v]$

$w_i = [(1-\delta_i)/\delta^{2i}] / \sum w_k$, with

$\delta_i = d_i/R$ for $d_i<R$

$w_i = 0$, otherwise

$d^2_i = f^2 NS. \{S^2+[v.(z_i- z_x)]^2\}$

$f NS = 1+ 0.03.|\Phi_i - \Phi_x|.[1+(\sin \Phi_i + \sin \Phi_x)/2]$

w_i : weight i

R : search radius (max. 2000 km)

s : horizontal (geodetic) distance [m]

i: Number of sites (maximum 6)

g_v: vertical gradient

w_k :sum of overall weights

v : vertical scale factor

z_x, z_i : altitudes of the sites [m]

i ,x: latitudes of the points

To meet current demands, it is no longer sufficient to rely solely on monthly average data. Many design codes now require hourly or minute data. However, due to the time-consuming nature of interpolating hourly values at arbitrary locations (a task that is only feasible with satellite data) and the need for extensive storage capacity, only interpolated monthly values at nodal points are stored. To generate hourly values at any desired location, stochastic models are used for global radiation. These models produce intermediate data that share the same statistical properties as the measured data, including average value, variance, and characteristic sequence (autocorrelation). The generated data aims to closely resemble the natural characteristics as much as possible. Recent research suggests that data generated using this method can effectively replace long-term measured data (Gansler et al., 1994).

The latest iteration of Markov Transition Matrices (MTM) can produce data for a broader range of climates by incorporating values clustered closely around the diagonal line, indicating minimal daily weather fluctuations. Two distinct models, namely the Perez model of 1991 and the Boland-Ridley-Lauret (BRL) model (Ridley et al., 2010), are available for accurately separating global radiation into beam and diffuse components.

The Perez dynamic model converts global hourly horizontal radiation values into hourly direct normal radiation values by incorporating parameters that characterize sky conditions. It necessitates the input of time series data for global radiation values and can incorporate dew point temperature within its calculations.

The Hofmann minute model can generate one-minute global irradiance time series using hourly averaged datasets. The algorithms begin by creating characteristic transition probability matrices (TPM) for various weather conditions (such as cloudless, broken clouds, and overcast) based on a vast amount of high-resolution measurements. Once the algorithms are set up, they are location-independent and can produce one-minute values by extrapolating from hourly averaged global irradiance data for any specified location.

The Skartveit and Olseth minute model was designed for generating data spanning 1 to 10 minutes and can be utilized with minimal modifications. The only adjustment made was in the methodology for generating time series. Instead of rearranging minute values to align with a specified autocorrelation value, the time series is now modeled using a straightforward autoregressive model (AR1) and subsequently matched with the calculated distribution.

2. Study area– Port Harcourt

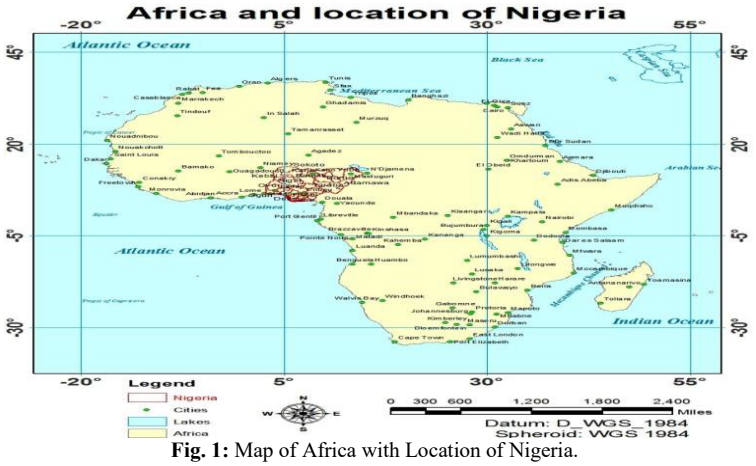

Fig. 1: Map of Africa with Location of Nigeria.

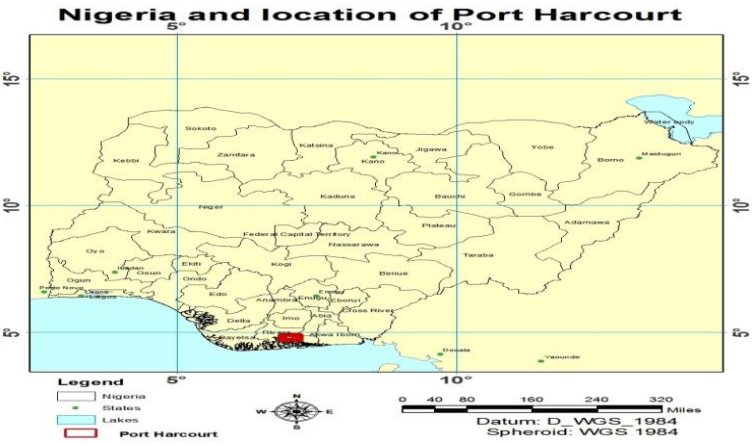

Fig. 2: Map of Nigeria with Location of Port Harcourt.

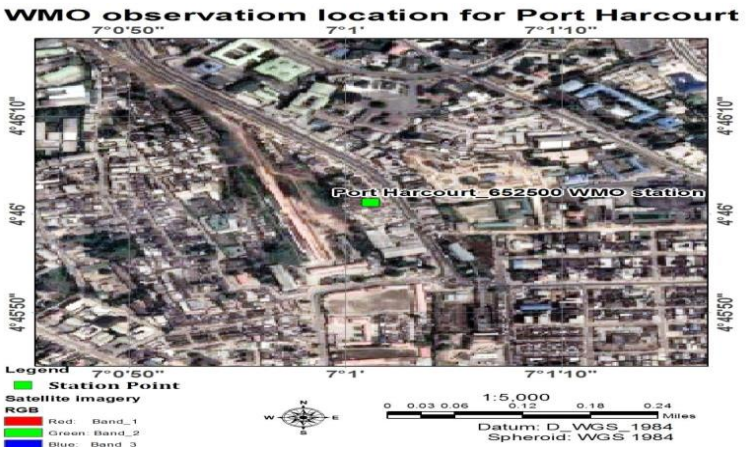

Fig 3: Map of WMO Location of Port Harcourt.

The research was conducted in Port Harcourt Metropolis, Rivers State, Nigeria, situated between latitudes 4°51' 30''N and 4° 57' 30''N and longitudes 6°50' 00''E and 7°00' 00''E. Port Harcourt is bordered by the Atlantic Ocean to the south, Bayelsa and Delta States to the west, Imo, Abia, and Anambra States to the north, and Akwa Ibom State to the east. The metropolis is in the sub-equatorial region and experiences a tropical climate with an average temperature of 30 °C, relative humidity ranging from 80% to 100%, and an annual rainfall of approximately 2,300mm (Mmom and Fred-Nwagwu, 2013). The primary Air Mass System observed in Rivers State is the Tropical Maritime Air Mass (mT), characterized by its high humidity and moisture content, which results in rainfall and is commonly referred to as the SW Monsoon Wind. The Tropical Continental (cT) air mass has a minimal impact, bringing harmattan conditions between December and February, known as the NE Trade Wind. These air masses are believed to play a role in the distribution of pollution in port-Harcourt. The inland areas of Rivers State are covered by tropical rainforest, while mangrove swamps dominate the coastal regions along the Atlantic Ocean. This vegetation represents one of the most lush, complex, and diverse terrestrial ecosystems on Earth (Eludoyin et al., 2013).

3. Methodology

The data on radiation, temperature, and precipitation for Port Harcourt World Meteorological Organisation (WMO) stations were sourced from the Meteonorm Version 8 database archives. Additional data from the National Climatic Data Center (USA) and the GEBA Global Energy Balance Archive were also utilized. This information was obtained using standard interpolation techniques, specifically Shepard's gravity interpolation model, with a North-South distance penalty applied. Monthly vertical scale factors and gradients were incorporated into the radiation interpolation process. Stochastic models and the Perez Tilt radiation model method were employed to analyze climate data from the periods of 1972–1991 and 1965–1989, focusing on temperature, radiation, and precipitation. Projections for 2050 and 2100 were carried out using radiation, temperature, and precipitation models. The coordinates for the Port Harcourt station are Latitude 4.767°N and Longitude 7.017 °E, with a location code number of 652500 and an altitude of 15m within the WMO climate network.

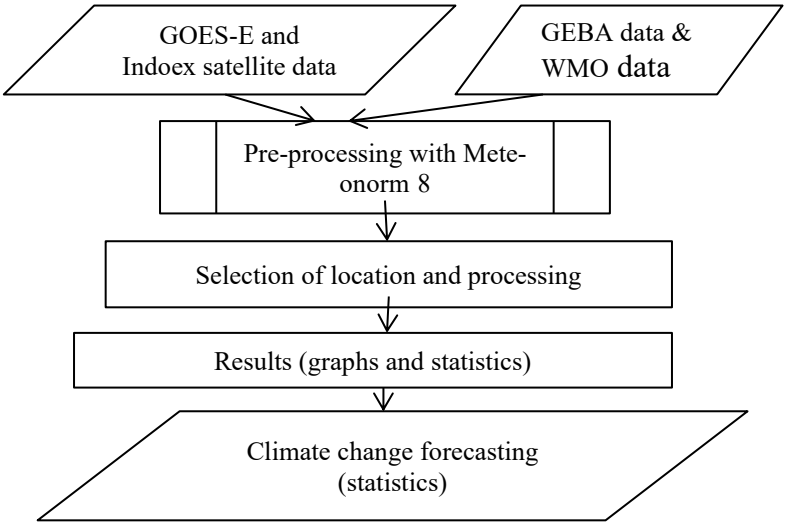

Fig 4: Methodology Workflow.

4. Results

The results were calculated using data from historical periods of 1972–1991, 1965–1989, and 2020, with projections made for the year 2050.

4.1. Meteorological parameters for 1972–1991 and 1965–1989

In this section, the results of the Standard temperature model for the temperature period 1972–1991, as well as the Perez radiation model for the radiation period 1965–1989 at WMO Port Harcourt station, are presented (see Table 1a &1b and figure 5-10). The uncertainty of yearly values is as follows: Gh (4%), Bn (7%), and Ta (0.3 °C), with a variability of Gh per year at 5.6%

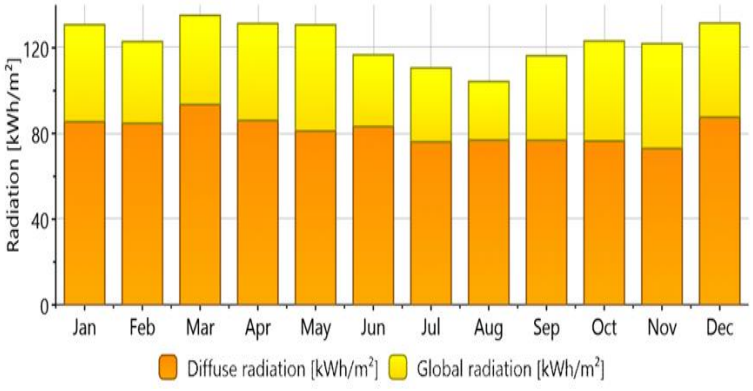

Fig. 5: Monthly Radiation from 1965–1989.

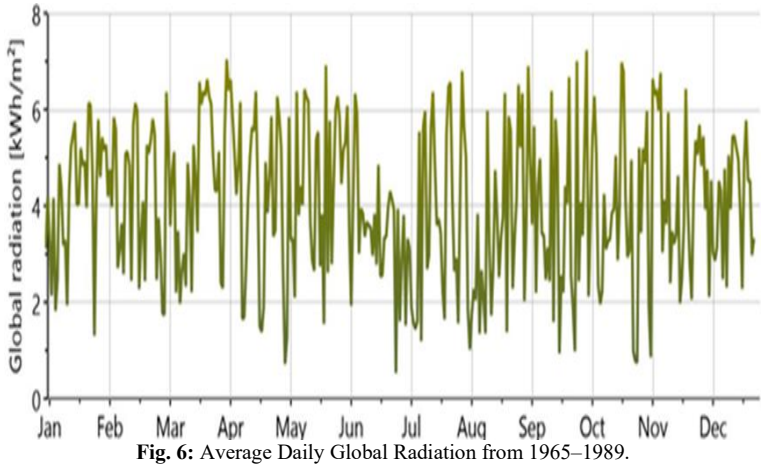

Fig. 6: Average Daily Global Radiation from 1965–1989.

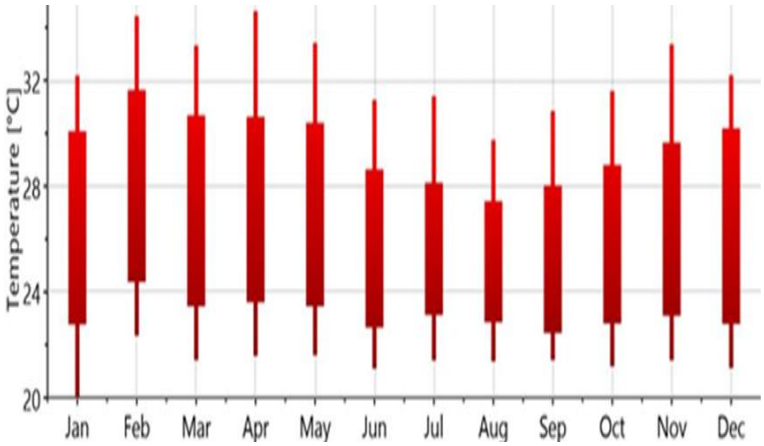

Fig. 7: Average Monthly Temperature Boxplot from 1972–1991.

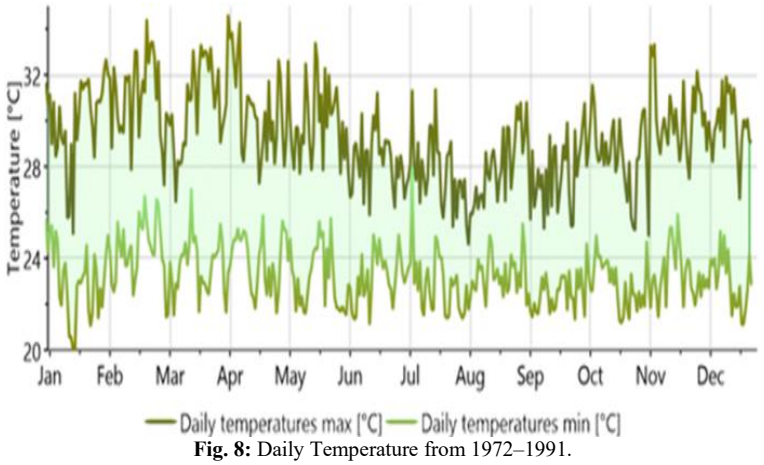

Fig. 8: Daily Temperature from 1972–1991.

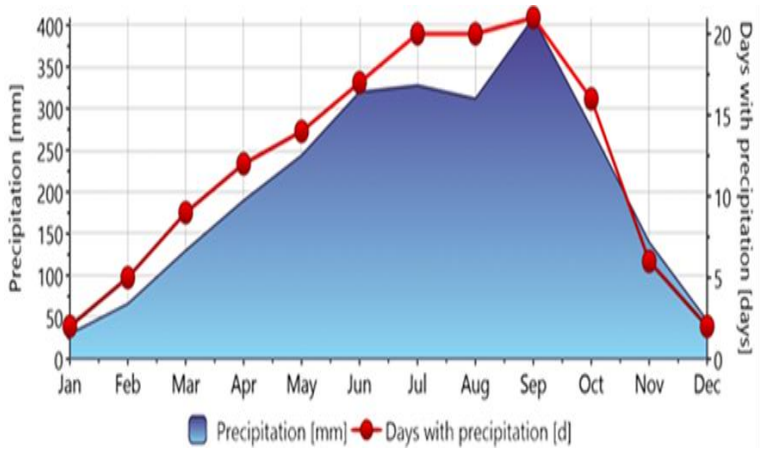

Fig. 9: Precipitation from 1972–1991.

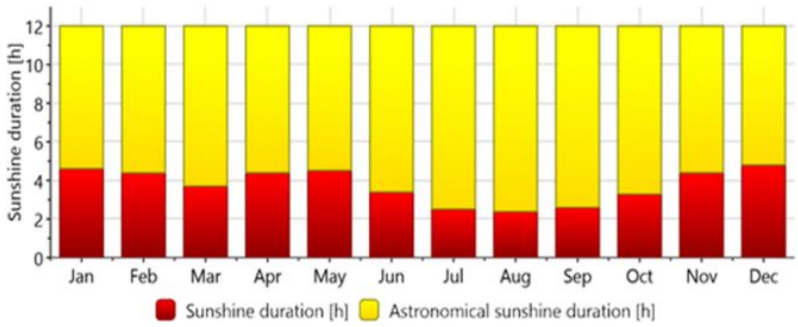

Fig. 10: Sunshine Duration from 1965–1989.

Table 1: A) Average Monthly Value for 1972–1991 and 1965–1989

Month	H_Gh [kWh/m^2]	H_Bn [kWh/m^2]	H_Dh [kWh/m^2]	Lg [lux]	Ld [lux]	N [octas]	Ta [°C]	Td [°C]
January	131	63	85	19532	14710	5	26.2	22.3
February	123	47	85	20392	15876	5	27.6	23.4
March	135	52	94	20452	16031	5	26.8	23.4
April	131	60	86	20600	15552	5	27.3	24.2
May	131	69	81	19851	14233	5	26.8	23.7
June	117	47	83	18337	14397	6	25.9	23.5
July	111	47	76	16802	12773	6	25.4	23.0
August	104	38	77	15953	12817	7	25.1	23.1
September	116	56	77	18377	13484	6	25.6	23.2
October	123	67	76	18760	13012	6	25.6	22.8
November	122	73	73	19202	13178	5	26.5	23.8
December	132	64	88	19802	15142	4	26.2	22.3
Year	1476	682	981	19005	14267	6	26.3	23.2

Table 1:B) Average monthly Value for 1972–1991 and 1965–1989

Month	RH [%]	p [hPa]	DD [deg]	FF [m/s]
February	78	1011	213	2.2
March	82	1011	210	2.2
April	83	1011	202	2.3
May	83	1011	197	2.3
June	87	1011	207	2.1
July	87	1011	215	2.1
August	89	1011	218	2.2
September	87	1011	214	2.1
October	85	1011	202	1.9
November	85	1011	200	1.6
December	79	1011	210	1.7
Year average	84	1011	209	2.1

Table 2: A) Average Monthly Values for 2020

Month	H_Gh [kWh/m^2]	H_Bn [kWh/m^2]	H_Dh [kWh/m^2]	Lg [lux]	Ld [lux]	N [octas]	Ta [°C]	Td [°C]
January	149	77	93	22199	16399	4	27.7	23
February	126	50	86	20900	16322	4	28.2	24.2
March	147	58	100	22177	17291	5	27.9	24.7
April	156	84	91	24333	17199	4	27.4	24.6
May	151	90	87	22871	15423	5	27.2	24.5
June	120	62	75	18761	13568	6	26.1	23.9
July	131	59	88	19854	14909	6	25.3	23.4
August	134	76	79	20402	13864	5	25	23.2
September	137	76	85	21528	15269	6	25.5	23.6
October	150	100	80	22793	14254	5	26	23.8
November	138	86	79	21592	14913	5	26.8	24.3
December	147	85	88	22029	16002	3	27.4	23.7
Year	1686	903	1030	21620	15451	5	26.7	23.9

Table 2: B) Average Monthly Values for 2020

Month	RH [%]	p [hPa]	DD [deg]	FF [m/s]
February	76	1011	213	1.2
March	79	1011	213	1.4
April	83	1011	210	1.6
May	85	1011	202	1.4
June	85	1011	197	1.4
July	88	1011	207	1.4
August	89	1011	215	1.5
September	90	1011	218	1.6
October	89	1011	214	1.4
November	88	1011	202	1.3
December	86	1011	200	1.2
Year average	80	1011	210	1.1

Table 3: A) Average Monthly Projected Values for 2050

Month	H_Gh [kWh/m^2]	H_Bn [kWh/m^2]	H_Dh [kWh/m^2]	Lg [lux]	Ld [lux]	N [octas]	Ta [°C]	Td [°C]
January	149	77	93	22199	16399	4	27.7	23
February	126	50	86	20900	16322	4	28.2	24.2
March	147	58	100	22177	17291	5	27.9	24.7
April	156	84	91	24333	17199	4	27.4	24.6
May	151	90	87	22871	15423	5	27.2	24.5
June	120	62	75	18761	13568	6	26.1	23.9
July	131	59	88	19854	14909	6	25.3	23.4
August	134	76	79	20402	13864	5	25	23.2
September	137	76	85	21528	15269	6	25.5	23.6
October	150	100	80	22793	14254	5	26	23.8
November	138	86	79	21592	14913	5	26.8	24.3
December	147	85	88	22029	16002	3	27.4	23.7
Year	1686	903	1030	21620	15451	5	26.7	23.9

Table 3: B) Average Monthly Projected Values for 2050

Month	RH [%]	p [hPa]	DD [deg]	FF [m/s]
February	76	1011	213	1.2
March	79	1011	213	1.4
April	83	1011	210	1.6
May	85	1011	202	1.4
June	86	1011	197	1.4
July	88	1011	207	1.4
August	89	1011	215	1.5
September	91	1011	218	1.6
October	90	1011	214	1.4
November	88	1011	202	1.3
December	87	1011	200	1.2
Year average	80	1011	210	1.1

4.2. Variability of meteorological parameters for 2020

In this section, the results for the Standard temperature model for the 2020 temperature period and the Perez radiation model for the 2020 radiation period for the WMO Port Harcourt station are determined (see Table 2a &2b and figure 11-16). The uncertainty of yearly values is as follows: Gh = 4%, Bn = 7%, Ta = 0.3 °C. The variability of Gh per year is 5.6%. The radiation interpolation locations include satellite data (100% of the share), and the temperature interpolation locations are Douala (312 km), Douala (312 km), and Douala (251 km).

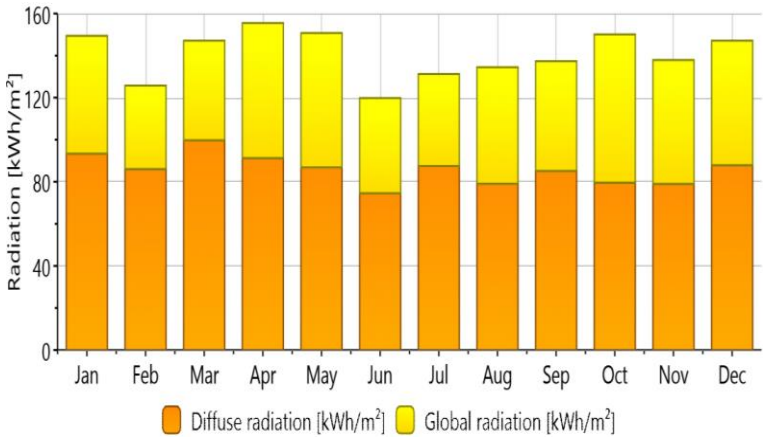

Fig. 11: Monthly Radiations for 2020.

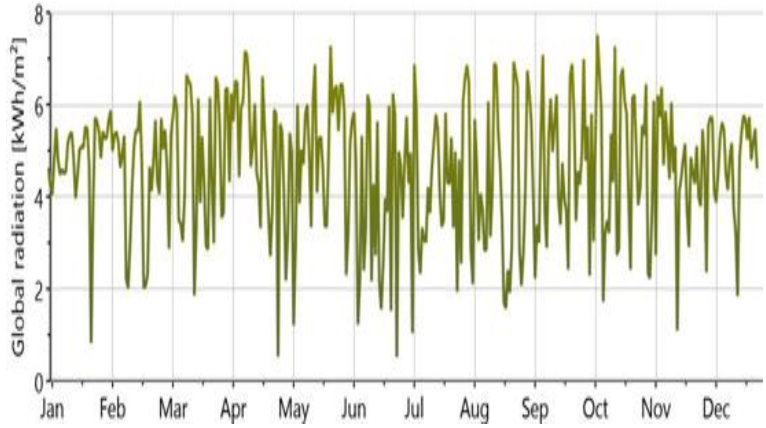

Fig. 12: Average Daily Global Radiations for 2020.

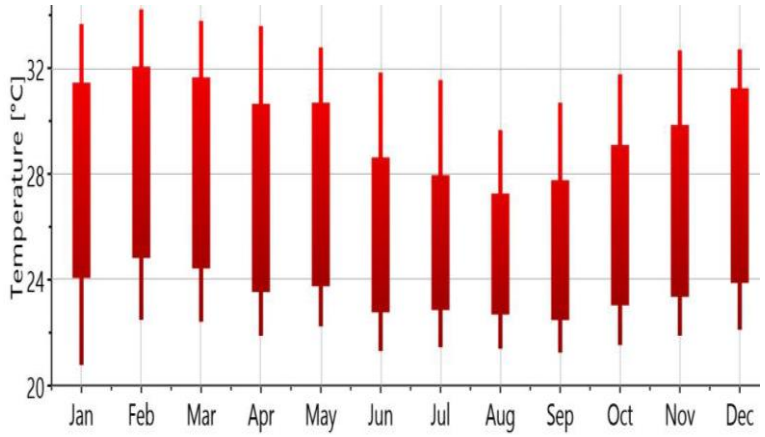

Fig. 13: Average Monthly Temperatures for 2020.

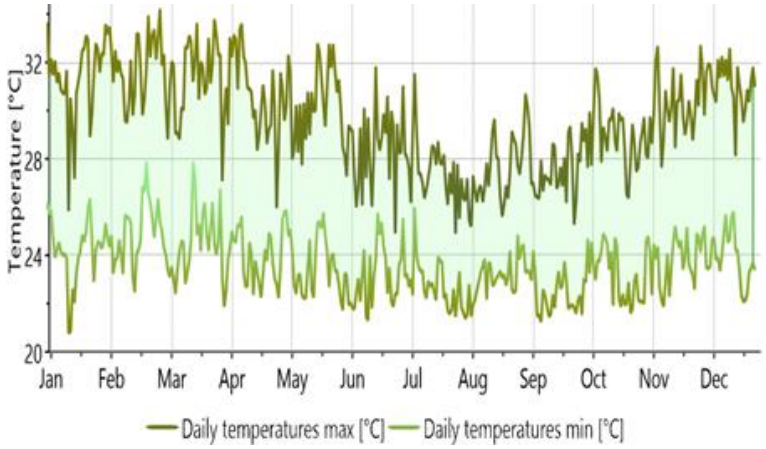

Fig. 14: Daily Temperatures for 2020.

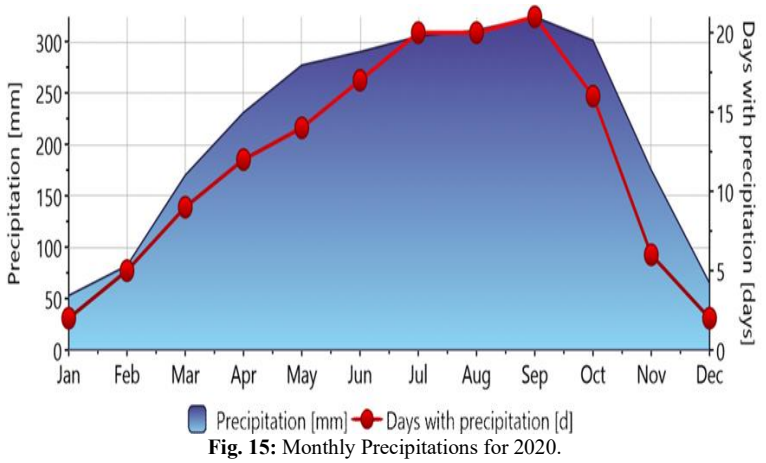

Fig. 15: Monthly Precipitations for 2020.

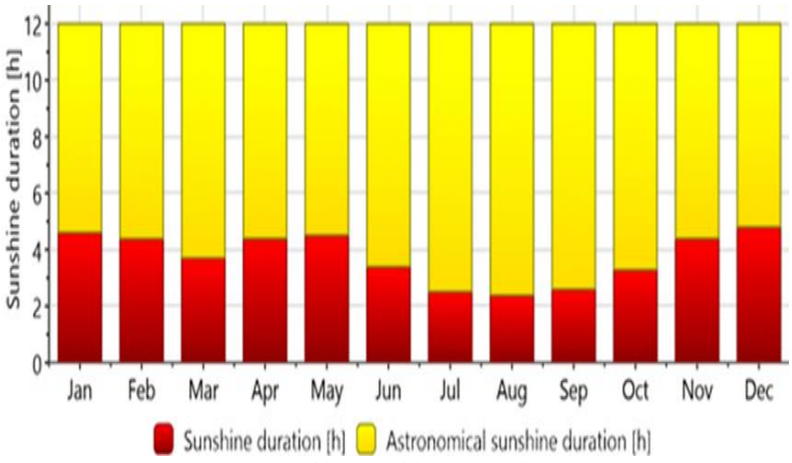

Fig. 16: Sunshine Monthly Duration for 2020.

4.3 Forecasting parameters for 2050

In this section, the result for the Standard Temperature model for Temperature forecasting for 2050 and the Perez radiation model. Radiation model for the radiation period of 20500 was determined for the WMO Port Harcourt station(see Table 3a &3b and figure 17-22). Uncertainty of yearly values: Gh = 4%, Bn = 7%, Ta = 0.3°C Variability of Gh / year: 5.6%. Radiation interpolation locations: Satellite data (Share of satellite data: 100%). Temperature interpolation locations: Douala (312 km), Douala (312 km), Benin City (251 km). The Representative Pathways Concentration (RPC) 2.6 for low was used. Forecasting Future Scenario: RPC 2.6.

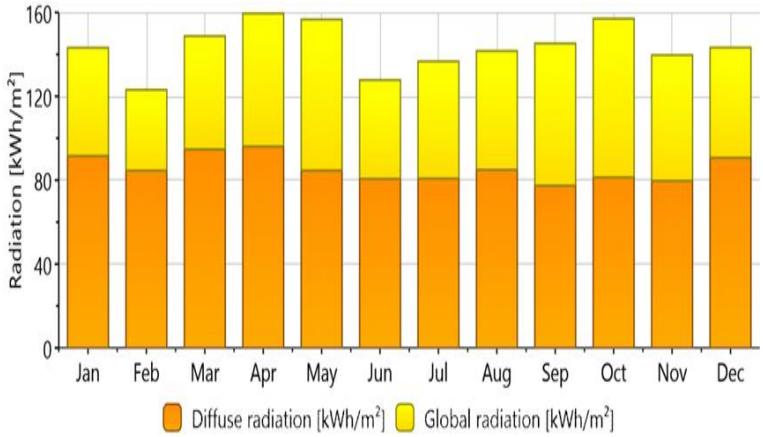

Fig. 17: Projected Monthly Radiations for 2050.

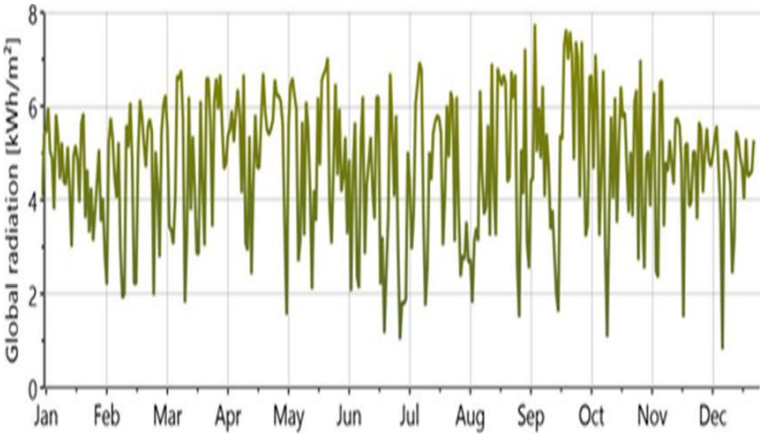

Fig. 18: Average Daily Projected Global Radiation for 2050.

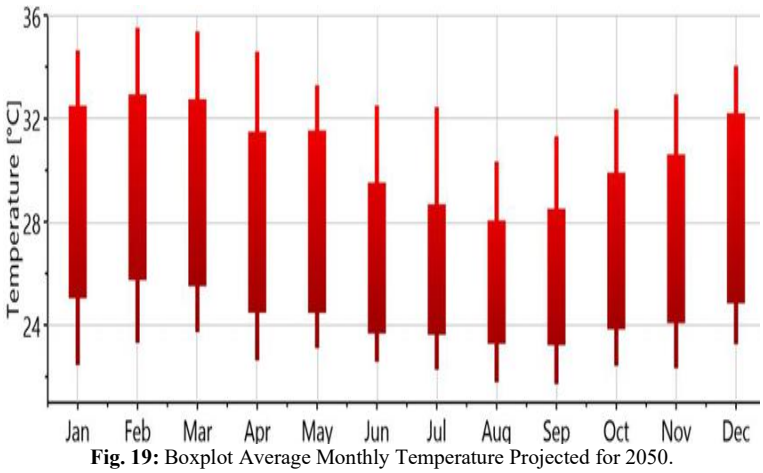

Fig. 19: Boxplot Average Monthly Temperature Projected for 2050.

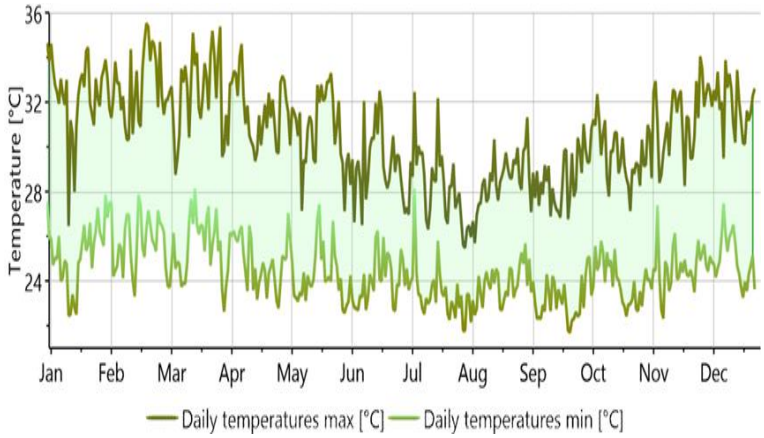

Fig. 20: Projected Daily Average Temperatures for 2050.

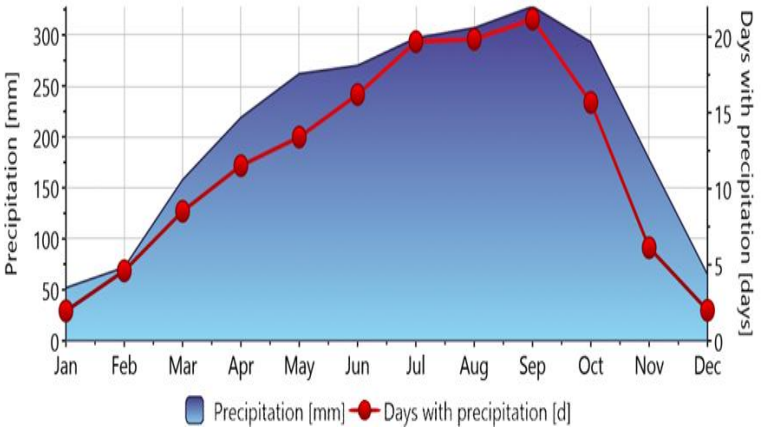

Fig. 21: Projected Monthly Precipitations for 2050.

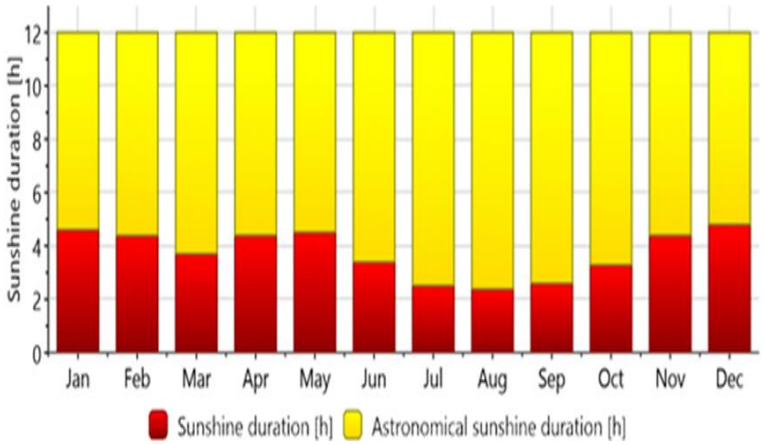

Fig. 22: Projected Monthly Sunshine Duration for 2050.

5. Discussion

The average monthly air temperature values for the period of 1972–1991 ranged from a maximum of 26.8°C in May and March to a minimum of 25.1°C in August, with an overall average of 26.3°C. The global horizontal irradiation for the years 1965–1989 reached a maximum of 135kWh/m2 in March and a minimum of 111 kWh/m2 in July, totaling 1476kWh/m2 for the year. The diffuse radiation horizontal irradiation for the same period peaked at 94kWh/m2 in March and dropped to 73kWh/m2 in November, with a yearly total of 981kWh/m2. The relative humidity ranged from a maximum of 89% in August to a minimum of 78% in February, with an average of 84%. The precipitation levels were at a maximum of 400mm in September and a minimum of 50mm in January during the period of 1972–1991. Sunshine hours averaged at five hours in December and two and a half hours in July for the years 1965–1989. The yearly average wind speed for the same period was 2.1 m/s.

In 2020, the average monthly air temperature ranged from a maximum of 28.2°C in February to a minimum of 25.0°C in August, with an overall average of 26.7°C. Global radiation horizontal irradiation peaked at 156kWh/m2 in April and reached a low of 120kWh/m2 in June, totaling 1686kWh/m2 for the year. Diffuse radiation horizontal irradiation had a maximum of 100kWh/m2 in March and a minimum of 75kWh/m2 in June, totalling 1030kWh/m2 for the year. The relative humidity in 2020 ranged from a maximum of 90% in August to a minimum of 76% in February, with an average of 85%. Precipitation reached a maximum of 323 mm in September and a minimum of 50mm in January for 2020. Sunshine hours varied, with a maximum of four and a half hours in December and an average of two hours in August.

In the forecast for the year 2050, the average monthly air temperature ranges from a maximum of 29.1°C in February to a minimum of 25.7°C in August, with an overall average estimate of 27.6°C. The projected global horizontal irradiation for 2050 is expected to reach a maximum of 160kWh/m2 in April and a minimum of 123kWh/m2 in February, with a total yearly estimate of 1722kWh/m2. The diffuse radiation horizontal irradiation for 2050 is forecasted to peak at 96kWh/m2 in April and drop to 77kWh/m2 in September, totaling 1027 kWh/m2 for the year. Relative humidity is expected to hit a high of 91% in August and a low of 76% in January, with an average of 85%. Precipitation for the year 2050 is projected to reach a maximum of 323 mm in September and a minimum of 50mm in January. Sunshine hours are estimated to peak at four and a half hours in December and average two hours in August.

The projected increases in temperature, shifts in rainfall patterns, and heightened frequency of extreme weather events are already exerting significant pressure on agriculture, water resources, human health, and biodiversity. The interconnectedness of these impacts underscores the urgent need for a holistic approach to climate action

In this study, data from various historical periods (1965-1989 and 1972-1991) were utilized for radiation, temperature, and precipitation analysis. The selection of these periods was based on data availability and considerations for ensuring consistent and comparable implications in line with the results obtained.

Meteonorm Version 8 is an indispensable tool for climate data provision, yet its accuracy in regions with sparse ground measurement networks is inherently limited by the reliance on interpolation from distant sites. This can significantly impact the precision of solar energy system design and performance prediction. Addressing this challenge requires a concerted research effort focused on increasing the density of reliable local weather data. By exploring innovative approaches such as low-cost sensor networks, citizen science, advanced geostatistical methods, and robust data fusion techniques, future developments can significantly enhance the spatial accuracy of tools like Meteonorm, leading to more resilient, efficient, and economically viable renewable energy projects worldwide.

6. Conclusion

Research findings indicate a rising trend in air temperature, relative humidity, pressure, and radiation levels. February, March, and April experience higher temperatures, as shown by meteorological data trends. A notable correlation exists between various metrics and air temperature. The expected reduction in precipitation in Port Harcourt from 400mm (1972–1991) to 323mm by 2050 is a significant observation. Similarly, global radiation levels are projected to increase from 1476kWh/m2 (1965–1989) to 1722kWh/m2 in 2050. The uncertainty in annual values for global radiation (Gh) is 4%, while for air temperature (Ta) it is 0.3°C. The variability of global radiation (Gh) is estimated to be 5.6% annually. When evaluating potential sites for green energy facilities like solar power stations and wind farms in Port Harcourt and Nigeria, it is important to consider historical data on both locations, as well as their climatic features. Utilizing various geographic models can help in this assessment process. Additionally, further research should be conducted on air temperature forecasting and radiation characteristics across the country to better understand and mitigate the impacts of climate change on livelihoods, habitats, environmental degradation, and induced migration

References

[1] Afrifa-Yamoah E.; I. Bashiru; I. Saeed and A. Karim. (2016). Sarima Modelling and Forecasting of Monthly Rainfall in the Brong Ahafo Region of Ghana. World Environment, 6(1): 1-9.

[2] Aweda, F. O. and Samson, T. K. (2020). Modelling the Earth's Solar Irradiance across Selected Station in Sub-Saharan Region of Africa. Iranian (Iranica) Journal of Energy and Environment Journal, 11(3): 204-211. https://doi.org/10.5829/IJEE.2020.11.03.05.

[3] Bohra-Mishra, P., Oppenheimer M. and S.M. Hsiang, (2014). Nonlinear permanent migration response to climatic variations but minimal response to disasters, Proceedings of the National Academy of Sciences (PNAS) 2014, 111, 27, 9780-9785. https://doi.org/10.1073/pnas.1317166111.

[4] Cai, R., Feng, S., Oppenheimer, M. and M. Pytlikova, (2016). Climate variability and international migration: the importance of the agricultural linkage. J. Environ. Econ. Manag. 79, 135–151, https://doi.org/10.1016/j.jeem.2016.06.005.

[5] Eludoyin O.S, Oderinde F.A, Azubuike O.J. (2013). Heavy metals concentration under rubber plantation (Hevea brasiliensis) in Hydromophic Soil of South-south.

[6] Frimpong, K.; J. Oosthizen and E. J. Van Etten. (2014). Recent trends in temperature and relative humidity in Bawku East, Northern Ghana. Journal of Geography and Geology, 6(2): 69 – 81. https://doi.org/10.5539/jgg.v6n2p69.

[7] Gansler, R.A., S.A. Klein and W.A. Beckman (1994): Assessment of the accuracy of generated meteorological data for use in solar energy simulation studies. Solar Energy, Vol. 53, No.3, pp. 279 - 287 https://doi.org/10.1016/0038-092X(94)90634-3.

[8] Geerts, B. (2003). Empirical estimation of the monthly-mean daily temperature range. Theoretical and Applied Climatology, 74: 145 – 165. https://doi.org/10.1007/s00704-002-0715-3.

[9] Gilgen H., M. Wild M., A. Ohmura (1998): Means and trends of shortwave incoming radiation at the surface estimated from Global Energy Balance Archive data. Journal of Climate, 11, 2042-2061. https://doi.org/10.1175/1520-0442-11.8.2042.

[10] Intergovernmental Panel on Climate Change. (2021). Climate Change 2021: The Physical Science Basis. Contribution of Working Group I to the Sixth Assessment Report of the Intergovernmental Panel on Climate Change. Cambridge University Press.

[11] Khatib, T. and Elmenreich, W. (2015). A model for hourly solar radiation data generation from daily solar radiation data using a generalized regression artificial neural network. International Journal of Photoenergy, 13(1): 1-13. https://doi.org/10.1155/2015/968024

[12] Khedhiri, S. (2015). Forecasting temperature record in PEI, Canada. Letters in Spatial and Resource Sciences, 9: 43-55, https://doi.org/10.1007/s12076-014-0135-x.

[13] Lefèvre, M., M. Albuisson and L. Wald (2002): Joint Report on Interpolation Scheme "Meteosat" and Database "Climatology I (Meteosat). SoDa Deliverable D3-8 and D5-1-4. Internal document.

[14] Lobell, D.B., G. I. Hammer; G. Mclean; C. Messina; M. J. Roberts and W. Schlenker. (2013). The critical role of extreme heat for maize production in the United States. Nature Climate Change, 3: 1-13. https://doi.org/10.1038/nclimate1832.

[15] Mmom P.C, Fred-Nwagwu F.W., (2013). Analysis of Landuse and Landcover Change around the City of Port Harcourt, Nigeria. Global Adv Res J Geogr Reg Plann 2: 076-86.

[16] Muhammet B. (2012). The analyse of precipitation and temperature in Afyonkarahisar (Turkey) in respect of Box-Jenkins technique. J. Academic Social Sci. Studies, 5(8): 196-212

[17] Murat, M; I. Malinowska; M. Gos and J. Krzyszczak. (2018). Forecasting daily meteorological time series using ARIMA and regression models. Int. Agrophys., 32: 253-264. https://doi.org/10.1515/intag-2017-0007.

[18] Poudyal, K. N.; B. K. Bhattarai; B. Sapkota and B. Kjeldstad. (2012). Estimation of global solar radiation using clearness index and cloud transmittance factor at trans-Himalayan region in Nepal. Energy and power Engineering, 4(6): 415 – 421. https://doi.org/10.4236/epe.2012.46055.

[19] Rebetez, M. (2001). Changes in daily and nightly day – to – day temperature variability during the twentieth century for two stations in Switzerland. Theoretical and Applied Climatology, 69(1 - 2): 13-21. https://doi.org/10.1007/s007040170032.

[20] Ridley, B., J. Boland, and P. Lauret (2010), Modelling of diffuse solar fraction with multiple predictors. Renewable Energy. 35(2): p. 478-483. https://doi.org/10.1016/j.renene.2009.07.018.
[21] Semenov M.A. and Shewry P.R. (2011). Modelling predicts that heat stress, not drought, will increase vulnerability of wheat in Europe. Scientific Reports, 1: 66. https://doi.org/10.1038/srep00066.
[22] Semenza, J.C. and K. Ebi, (2019). Climate change impact on migration, travel, travel destinations and the tourism industry. Journal of travel medicine vol. 26,5 (2019): taz026. https://doi.org/10.1093/jtm/taz026
[23] Ukhurebor, K. E.; T. B. Batubo; I. C. Abiodun and E. Enoyeze. (2017). The influence of air temperature on the dew point temperature in Benin City, Nigeria. Journal of Applied Sciences and Environmental Management, 21(4): 657-660. https://doi.org/10.4314/jasem.v21i4.5.
[24] Wald, L. and M. Lefèvre (2001): Interpolation schemes - Profile Method (a process-based distance for interpolation schemes). SoDa Deliverable D5-1-1. Internal document
[25] World Meteorological Organisation (WMO) (1998): 1961 – 90 Climatological Normals (Clino). Version 1.0 – November 1998.
[26] Yousif, T. A. and Tahir, M. H. (2013). The relationship between relative humidity and dew point temperature in Khartoum State, Sudan. Journal of Applied and Industrial Sciences, 1(5): 20 – 23.
[27] Zelenka, A., G. Czeplak.,V. D'Agostino, J. Weine., E. Maxwell., R. Perez, M. Noia, C. Ratto and R. Festa (1992): Techniques for supplementing solar radiation network data, Volume 1-3. IEA Report No.IEA-SHCP-9D-1.